Australian Journal of Earth Sciences (2003) **50**, 853–864

Revised geochronology of magmatism in the western Capricorn Orogen at 1805–1785 Ma: diachroneity of the Pilbara–Yilgarn collision

D. A. D. EVANS,[1]* K. N. SIRCOMBE,[2] M. T. D. WINGATE,[2] M. DOYLE,[3] M. McCARTHY,[4] R. T. PIDGEON[4] AND H. S. VAN NIEKERK[5]

[1]*Department of Geology and Geophysics, Yale University, PO Box 208109, New Haven CT 06520–8109, USA.*
[2]*Tectonics Special Research Centre, University of Western Australia, 35 Stirling Highway, Crawley, WA 6009, Australia.*
[3]*Geological Survey of Western Australia, 100 Plain Street, East Perth, WA 6004, Australia.*
[4]*School of Applied Geology, Curtin University of Technology, GPO Box U1987, Perth, WA 6845, Australia.*
[5]*Department of Geology, Rand Afrikaans University, Auckland Park 2006, Johannesburg, South Africa.*

The June Hill Volcanics occupy a central stratigraphic position in the tectonic evolution of the Capricorn Orogeny that occurred along the southwestern margin of the Pilbara Craton in Palaeoproterozoic time. The volcanic rocks have been interpreted alternatively as due to continental rifting, foreland-basin development, or backarc extension. Previous multigrain zircon U–Pb results from these rocks, as well as from an unnamed rhyolitic porphyry that is interstratified in turbidites of the overlying Ashburton Formation, are influenced by the combined effects of Pb loss and xenocrystic inheritance. We report new SHRIMP zircon ages of 1799 ± 8 and 1786 ± 11 Ma, respectively from the June Hill Volcanics and the unnamed porphyry, both of which have been deformed during the Capricorn Orogeny. Close similarity between these ages and results from various late-stage Capricorn granitoids (including our new SHRIMP result of 1795 ± 8 Ma for the Minnie Creek granite) imply rapid development of the western Ashburton Trough, accumulating and deforming ~10 km of turbiditic sediments in about 10 million years. Comparison of our new June Hill age with previous SHRIMP results from the central Ashburton Trough implies that foreland-basin development of the Capricorn Orogeny was significantly diachronous, younging westward during oblique Pilbara–Yilgarn convergence.

KEY WORDS: Ashburton Trough, Capricorn Orogen, geochronology, Palaeoproterozoic, SHRIMP, uranium–lead dating.

INTRODUCTION

The Capricorn Orogen (Figure 1) delineates convergence between the Pilbara and Yilgarn Cratons in Western Australia (Tyler & Thorne 1990; Thorne & Seymour 1991), with an extensive supracrustal record preserved in the Ashburton Fold Belt (Gee 1979; Tyler & Thorne 1990) on the southern and western margins of the Pilbara Craton. Although the timing and character of earlier events in the orogen's evolution are contentious (Krapez 1999; Martin *et al*. 2000), its terminal developments (the Capricorn Orogeny: Occhipinti *et al*. 1998, 1999) are more clearly defined by recent U–Pb SHRIMP ages of *ca* 1800 Ma throughout the Ashburton Fold Belt and adjacent internides, the Gascoyne Complex (Nelson 1995, 1998, 1999, 2000, 2001; Pearson 1996; Occhipinti *et al*. 1998; Krapez & McNaughton 1999; Hall *et al*. 2001).

Sedimentary and volcanic strata of the upper Wyloo Group (Figures 1, 2) document much of the orogenic development within the Ashburton Fold Belt (Tyler & Thorne 1990; Thorne & Seymour 1991; Krapez 1999). Among its northwestern exposures in the Duck Creek region, north of Wyloo Dome, this succession comprises a basal conglomerate and sandstone association (Mt McGrath Formation), a carbonate platform (Duck Creek Dolomite), locally preserved volcanic rocks (June Hill Volcanics) and a thick turbiditic succession with sporadic interbeds of iron-formation (Ashburton Formation). The upper Wyloo Group has been interpreted in fundamentally different tectonic environments (Figure 2). Tyler and Thorne (1990) and Thorne and Seymour (1991) postulated a foreland-basin setting for the entire Wyloo Group, deposited on the lower plate of an eventual continent–continent collision. In contrast, Powell and Horwitz (1994) ascribed an extensional, rift–drift environment to the Mt McGrath Formation, Duck Creek Dolomite and June Hill Volcanics. Krapez (1997a), 1999) proposed that rifting was established prior to Mt McGrath sedimentation, and an abrupt transition between divergent and convergent continental-margin regimes is precisely marked by the onset of June Hill volcanism. In this model the June Hill Volcanics erupted within a backarc basin behind a west-facing arc (in present coordinates) with the Pilbara Craton lying in the upper plate of the subduction zone.

*Corresponding author: dai.evans@yale.edu

Previous conventional (multigrain thermal-ionisation mass spectrometry) U–Pb zircon ages from the June Hill Volcanics would appear to constrain tightly the evolution of the uppermost Wyloo Group, yet differences in interpretation of these ages remain. In reporting these ages, Pidgeon and Horwitz (1991) emphasised the broad similarity between their results from the 1843 ± 2 Ma *in situ* June Hill Volcanics, and 1828 ± 38 Ma felsic volcanic rocks (quartz–feldspar-phyric porphyry and tuffaceous units) interstratified among the western exposures, and thus presumably within the upper part, of the Ashburton Formation. In their interpretation, the porphyries are representative of a number of olistoliths derived from the June Hill volcanic episode and redeposited downslope amid turbidite sedimentation. This model has been questioned by Krapez (1997b, 1999) who postulated that the porphyries lie within structurally intact sections of the June Hill and adjacent sequences, whose diverse distribution of exposure is dictated merely by Capricorn folding and faulting. Limited exposure allows for many interpretations of these isolated igneous units.

Hall *et al.* (2001) have reported a sensitive high-resolution ion microprobe (SHRIMP) U–Pb zircon age of 1804 ± 7 Ma from the Capricorn Formation, a fluvial-dominated succession unconformably overlying deformed Ashburton Formation turbidites in the Capricorn Range and nearby locations (Figure 1). Assuming correlatability of the Ashburton turbidites between that area and the Duck Creek region, the combined U–Pb results would thus indicate moderately rapid tectonic development of the Ashburton Fold Belt between *ca* 1845 and 1805 Ma (see discussion in Hall *et al.* 2001).

However, despite the high precision quoted for the conventional U–Pb ages from the Duck Creek area (Pidgeon & Horwitz 1991), some unsettling features of the data remain unresolved. For example, the upper intercept result of 1843 ± 2 Ma from *in situ* June Hill Volcanics incorporated only four of the five multigrain analyses; if the age is correct then the fifth sample, discordant with a $^{207}Pb/^{206}Pb$ age of 1928 ± 5 Ma, would appear to indicate some combination of xenocrystic inheritance and secondary isotopic disturbance. As all five analyses are isotopically discordant, such an interpretation invites consideration that they too may suffer from minor xenocrystic inheritance. Similar difficulties affect the zircon analyses from the alleged olistoliths (Pidgeon & Horwitz 1991).

In an effort to clarify the temporal framework of the upper Wyloo Group, we have undertaken a U–Pb zircon

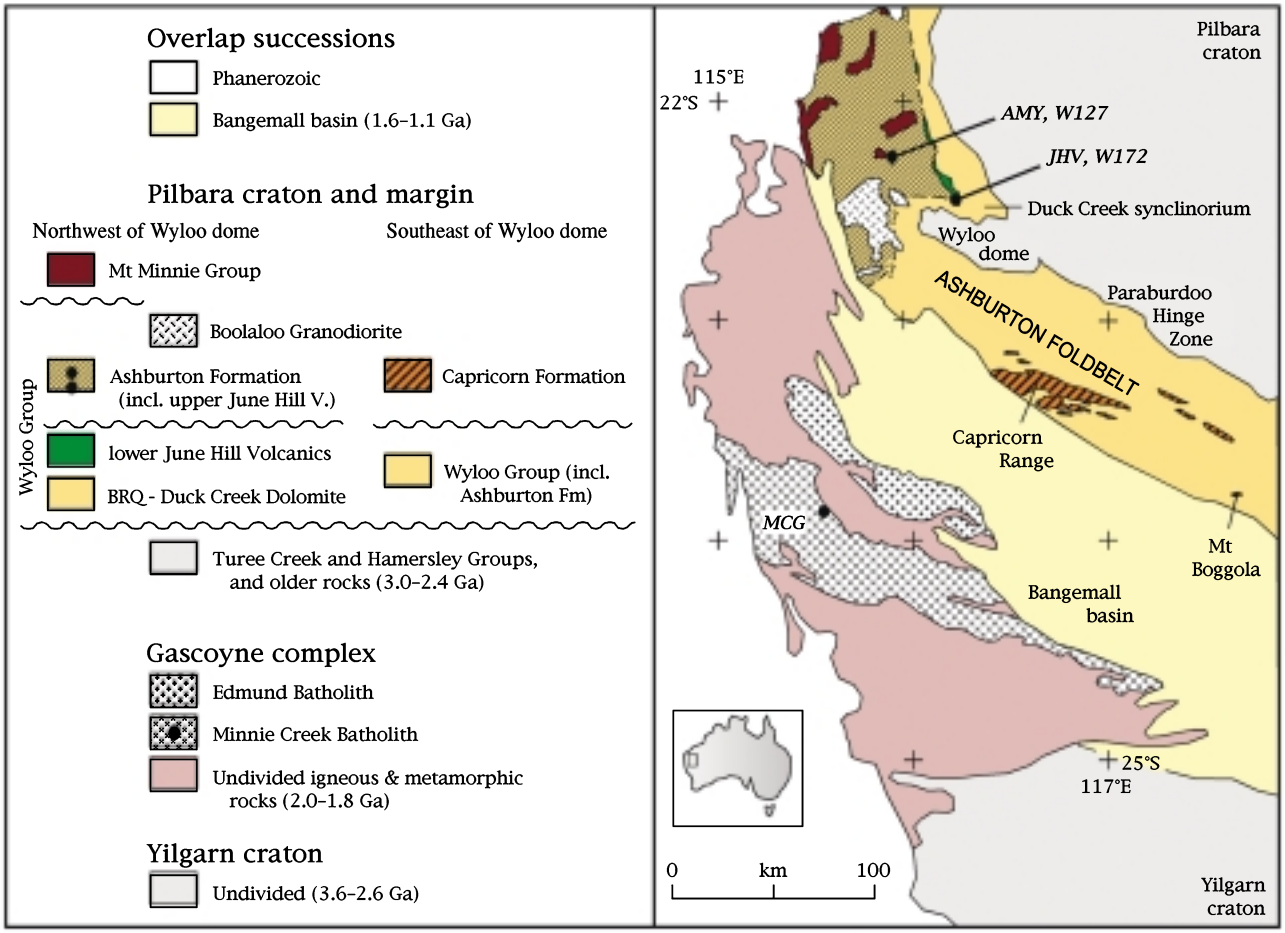

Figure 1 Lithostratigraphy of the western Capricorn Orogen. Rocks dated in this study are marked by black dots. BRQ, Beasley River Quartzite at base of the Wyloo Group. Note that in the region northwest of the Wyloo Dome, fine-grained siliciclastic rocks exist between the Duck Creek Dolomite and the upper June Hill Volcanics; these have been assigned to the Mininer Sequence by Krapez (1999).

study of the same rocks using the SHRIMP. This method provides the spatial resolution necessary for identification of sub-millimetre isotopic heterogeneity within individual grains, and hence can ascertain the sources of anomaly in the Pidgeon and Horwitz (1991) dataset. We also present new SHRIMP zircon data from the Minnie Creek granite, one of the late-stage granitoids in the Gascoyne complex (Williams 1986), which forms the internal zone of the Capricorn Orogen. Our results carry important implications for stratigraphic and tectonic development of the Capricorn Orogeny.

SAMPLING AND METHODS

We report SHRIMP analyses of five zircon samples from three stratigraphic units: the June Hill Volcanics, an unnamed quartz–feldspar (dacitic) porphyry east of Mt Amy and the Minnie Creek granite. Sample JHV is from the June Hill Volcanics near the type locality in the Duck Creek synclinorium (Figure 1; see Table 1 for precise locality coordinates). The present study has been undertaken in conjunction with research on the stratigraphy and physical volcanology of the June Hill Volcanics (McCarthy 2001). That work has recognised an angular unconformity within the June Hill Volcanics as presently mapped (Seymour *et al*. 1988), and sample JHV has been taken from above the unconformity. The rock is a clast-supported, non-welded pumice breccia–sandstone. The fragment population comprises mainly feldspar>quartz-phyric pumice clasts and crystal fragments (principally quartz, plagioclase, orthoclase), suggesting a rhyolitic to rhyodacitic composition. Pumice clasts are mostly elongate with irregular shapes and have relict uncompacted round and tube vesicle texture in quartz-altered domains. Angular to subrounded dolomite clasts, up to 3 m in length and strikingly similar in lithology to uppermost strata of the Duck Creek Dolomite, were avoided during sampling. The lithofacies characteristics of the pumice-bearing sandstone are consistent with aggradation from large-volume subaqueous gravity flows of pyroclastic and non-volcanic detritus (McCarthy 2001).

Sample W172 consists of a duplicate fraction of the low-magnetic, 74–105 μm zircon concentrate previously processed in the study by Pidgeon and Horwitz (1991). Unfortunately, with the passing of R. C. Horwitz, all detailed field notes, bulk specimens and thin-sections of this sample have been lost. Nonetheless, we believe that W172 is from the same stratigraphic unit as our JHV sample, because the pumice breccia–sandstone is the only likely source of primary magmatic zircons in the map area. As will be shown below, indistinguishable U–Pb ages from the two samples support this conclusion.

Sample AMY is taken from the dacitic porphyry that crops out 7 km east of Mt Amy, as described by Thorne and Seymour (1991: p. 83). Sample W127 is a duplicate fraction of low-magnetic, 105–135 μm zircon concentrate previously processed in the work by Pidgeon and Horwitz (1991). In

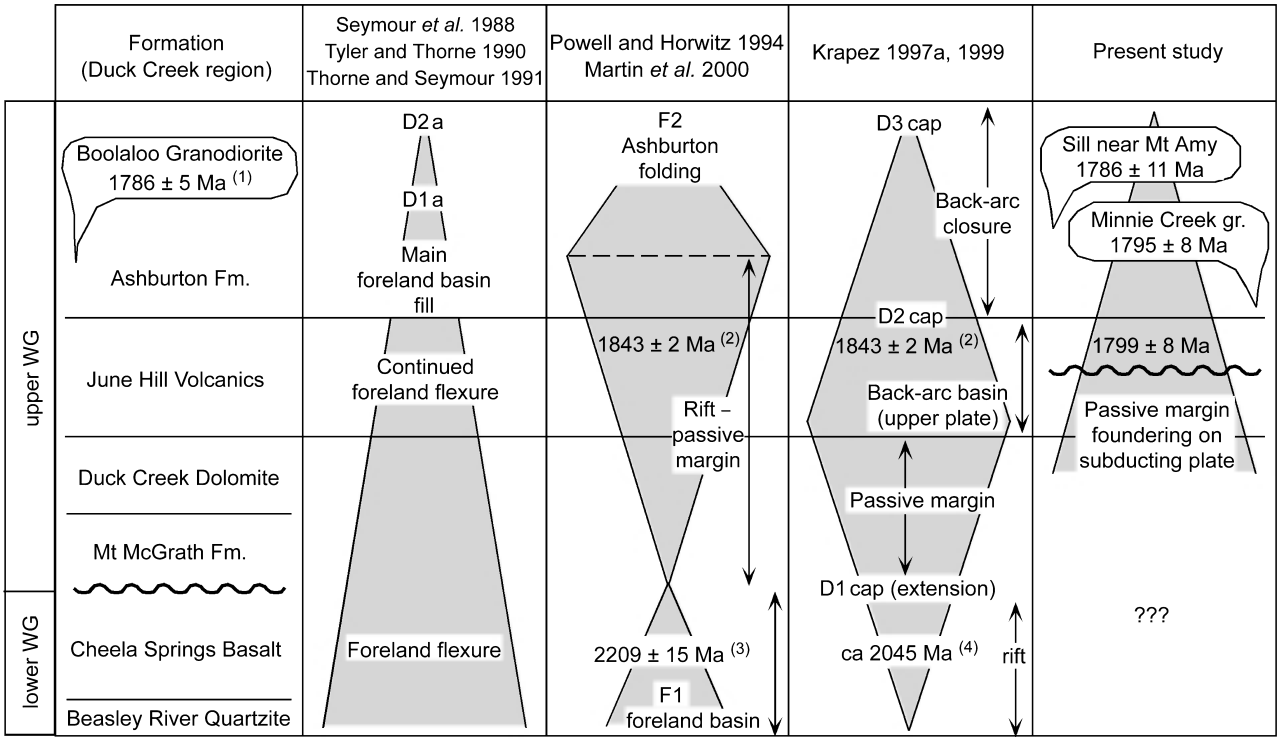

Figure 2 Varying tectonic interpretations of the Wyloo Group. Widths of shaded regions schematically represent stages of proposed Wilson cycle evolutions; thickening upward = divergence, thinning upward = convergence. Lithostratigraphy applies to Duck Creek region only; see note to Figure 1. Sources of quoted ages: 1, SHRIMP U–Pb zircon, Krapez and McNaughton (1999); 2, conventional U–Pb zircon, Pidgeon and Horwitz (1991); 3, SHRIMP U–Pb zircon, Martin *et al*. (1998); 4, prediction from assumed supercontinental periodicity, Krapez (1997a), 1999). The Minnie Creek granite intrudes presumed metamorphic equivalents of the Wyloo Group (Williams 1986).

this instance there is no question that AMY is taken from the same stratigraphic unit as sample W127 of Pidgeon and Horwitz (1991), as the sample coordinates described in that study lead directly to exposures of the distinctive porphyry. Again, indistinguishable U–Pb results from the two samples verify that they are from the same formation

The Minnie Creek sample (MD02MC) consists of coarse-grained biotite (now chlorite) granite of the Minnie Creek Batholith. The rock is most closely related to the 'massive central granodiorite' phase of the batholith as described by Williams (1986); the sampled outcrop lies in a small enclave of this phase within the otherwise foliated marginal phase of the batholith.

Zircon grains were extracted from the three new samples using standard crushing, heavy-liquid and paramagnetic separation methods. Grains were then hand-picked, mounted in epoxy and polished to reveal half-sections. Optical and electron imaging was used to document possible internal grain structures and compositional heterogeneities. All samples displayed bland cathodoluminescence, but distinct regular zoning and occasionally prominent core/rim structures were observed with backscattered electron imaging.

Measurements of U, Th, and Pb were conducted using the Perth Consortium SHRIMP II ion microprobe at Curtin University of Technology. Decay constants employed are those recommended by Steiger and Jäger (1977). U–Th–Pb ratios and absolute abundances were determined relative to the CZ3 standard zircon [$^{206}Pb/^{238}U$ = 0.09143 (564 Ma), 550 ppm ^{238}U: Pidgeon *et al.* 1994; Nelson 1997], analyses of which were interspersed with those of unknown-aged grains, using operating and data processing procedures similar to those described by Compston *et al.* (1984, 1992), Claoué-Long *et al.* (1995) and Nelson (1997). Measured compositions were corrected for common Pb using non-radiogenic ^{204}Pb. Corrections are sufficiently small to be insensitive to the choice of common Pb composition, and an average crustal composition (Cumming & Richards 1975) appropriate to the age of the mineral was assumed. Analytical details are summarised in Table 2. Weighted mean ages for pooled analyses are reported with 95% confidence intervals, except where noted otherwise.

RESULTS

JHV: June Hill Volcanics

The zircons are euhedral, range up to ~300 μm in length, and have length to width ratios up to 4:1. Most are relatively transparent and range from colourless to pale brown. Euhedral concentric zoning is prominent in most crystals, although this appears diffused in parts and there are distinct indications of possible inherited zircon cores in some grains. Measured compositions are generally concordant (Figure 3a). Inheritance is revealed with two grains demonstrating significant difference between core and rim ages (13 core/rim: 2184/1933 Ma and 15 core/rim: 1922/1788 Ma). The range in $^{207}Pb/^{206}Pb$ suggests that inheritance is also an issue beyond the obvious core/rim structures seen in some grains and has not been entirely resolved by these analyses. Analysis 5.1 is reversely discordant although the reasons for this are not clear beyond a moderately elevated common Pb composition. Excluding significantly older analyses (3.1, 13.1, 13.2, 15.1) and 5.1, the weighted mean of $^{207}Pb/^{206}Pb$ ratios is 0.109991 ± 0.000219, equivalent to 1799.3 ± 3.6 Ma (1σ). The best estimate of the crystallisation age of this sample is 1799 ± 8 Ma (95% conf., MSWD: 1.4).

W172: replicate analysis of June Hill Volcanics

The zircons are euhedral, range up to ~200 μm in length, and have length to width ratios up to 4:1. These and all other optical features are similar to the JHV sample described above. Measured compositions are generally concordant (Figure 3b). Inheritance is seen in one grain (13 core/rim: 2404/1788 Ma). The range in $^{207}Pb/^{206}Pb$ is not as wide as the JHV sample, which suggests that inheritance is less of an issue among these analyses. Excluding one significantly older age (13.1) and a significantly discordant analysis (2.1), the weighted mean of $^{207}Pb/^{206}Pb$ ratios is 0.109845 ± 0.000223, equivalent to 1796.8 ± 3.7 Ma (1σ). The best estimate of the crystallisation age of this sample is 1797 ± 8 Ma (95% conf., MSWD: 1.2), indistinguishable from that of the JHV zircon concentrate.

AMY: unnamed porphyry 7 km east of Mt Amy

The zircons are euhedral, range up to ~250 μm in length, and have length to width ratios up to 3:1. Most are relatively transparent and range from colourless to pale brown. Euhedral concentric zoning is seen in most crystals, although this appears more strongly diffused in parts than the JHV sample and there are only rare indications of possible inherited zircon cores. Measured compositions are generally concordant although there is the suggestion of recent Pb-loss (Figure 3c). Inheritance is revealed with two analyses (7, 8) yielding significantly older ages at *ca* 1830 Ma. The range in $^{207}Pb/^{206}Pb$ is not as wide as the JHV sample, which suggests that inheritance is not as significant among these analyses. Analysis 12.1 is reversely discordant although the reasons for this are not clear beyond a moderately elevated common-Pb composition. Excluding significantly older ages (7.1, 8.1) and 12.1, the weighted mean of $^{207}Pb/^{206}Pb$ ratios is 0.109172 ±

Table 1 Sample locations (UTM coordinates referenced to GDA94).

Sample	Easting	Northing	1:50 000 map sheet
JHV (June Hill Volcanics)	424240	7514100	Urandy
AMY (unnamed porphyry)	392690	7536300	No.42 Well
Minnie Creek granite	351900	7359550	Mangaroon

For W172 and W127, see Pidgeon and Horwitz (1991) p.58.

0.000285, equivalent to 1785.6 ± 4.8 Ma (1σ). The best estimate of the crystallisation age of this sample is 1786 ± 11 Ma (95% conf., MSWD: 0.6).

W127: replicate analysis of unnamed porphyry

The zircons are euhedral, range up to ~300 μm in length, and have length to width ratios up to 3:1. As with the other samples, most of these grains are relatively transparent and bear prominent euhedral concentric zoning. Measured compositions are generally concordant (Figure 3d). Inheritance is not directly seen, although one analysis (16.1) is slightly more than 2σ from the mean of the group. The range in $^{207}Pb/^{206}Pb$ would also suggest that inheritance is an issue among these analyses. Excluding analysis 16.1, the weighted mean of $^{207}Pb/^{206}Pb$ ratios is 0.109431 ± 0.000267, equivalent to 1790.0 ± 4.5 Ma (1σ). The best estimate of the crystallisation age of this sample is 1790 ± 10 Ma (95% conf., MSWD: 0.8), indistinguishable from that of the AMY zircon concentrate.

MCG: Minnie Creek granite

The zircons are euhedral, range up to ~500 μm in length, and have length to width ratios up to 4:1. Most are relatively transparent and range from colourless to pale brown. Many contain small ovoid or tubiform fluid inclusions. Euhedral concentric zoning is prominent in most crystals, and there are no indications of the presence of inherited zircon cores. Measured compositions range from concordant to slightly normally discordant (Figure 3e). The $^{206}Pb/^{238}U$ ages are inversely correlated with U concentration, indicating that the zircons have undergone minor loss of radiogenic Pb associated with radiation damage. The $^{207}Pb/^{206}Pb$ ages do not correlate with U content, however, and are well grouped, indicating that Pb loss was

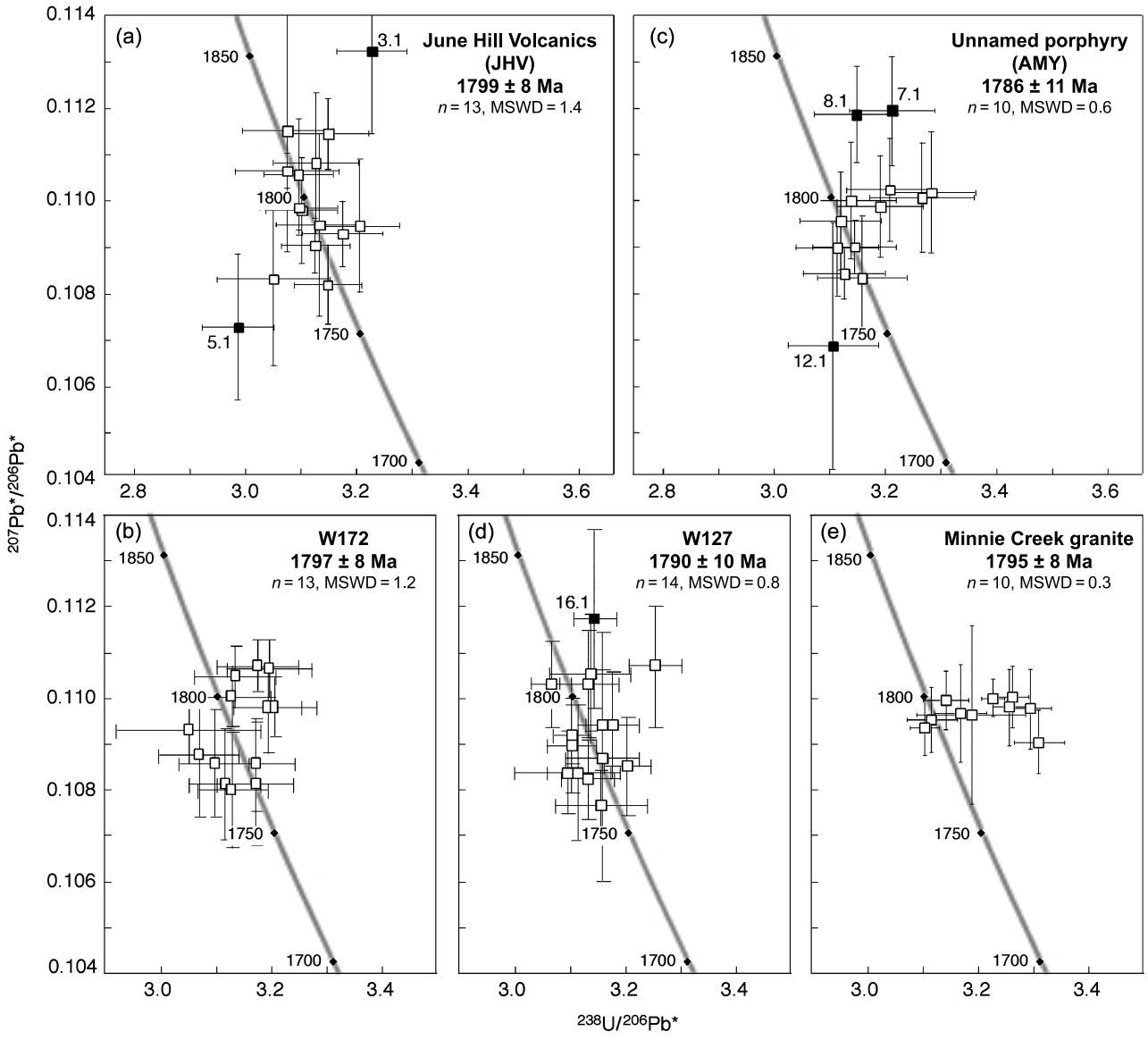

Figure 3 Tera-Wasserburg concordia diagrams of SHRIMP results from this study. Filled squares, labelled, represent analyses excluded from the mean age. Errors of measurements are 1σ; errors of means are 95% confidence.

Table 2 Summary of U–Pb analytical data.

Spot name	U (ppm)	Th (ppm)	Pb (ppm)	^{204}Pb (ppb)	^{204}Pb/^{206}Pb	f206	^{207}Pb/^{235}U	^{206}Pb/^{238}U	^{207}Pb/^{206}Pb	^{206}Pb/^{238}U Age (Ma)	^{207}Pb/^{206}Pb Age (Ma)	Conc. (%)
JHV-1.1	149	70	50	3	0.00007	0.00110	0.3120 ± 0.0070	4.708 ± 0.128	0.10947 ± 0.00143	1750.3 ± 34.4	1790.6 ± 24.0	97.8
JHV-2.1	171	87	60	1	0.00003	0.00045	0.3225 ± 0.0067	4.883 ± 0.119	0.10980 ± 0.00114	1802.0 ± 32.7	1796.1 ± 19.0	100.3
JHV-3.1[a]	277	135	94	76	0.00102	0.01633	0.3099 ± 0.0060	4.838 ± 0.128	0.11323 ± 0.00178	1740.2 ± 29.8	1851.9 ± 28.8	94.0
JHV-4.1	248	128	87	4	0.00005	0.00083	0.3231 ± 0.0065	4.926 ± 0.118	0.11057 ± 0.00119	1804.8 ± 31.7	1808.8 ± 19.6	99.8
JHV-5.1 [a]	126	112	49	7	0.00019	0.00302	0.3348 ± 0.0072	4.953 ± 0.136	0.10729 ± 0.00157	1861.7 ± 34.8	1753.9 ± 27.1	106.2
JHV-6.1	203	93	69	4	0.00006	0.00102	0.3177 ± 0.0062	4.740 ± 0.103	0.10820 ± 0.00085	1778.5 ± 30.2	1769.4 ± 14.4	100.5
JHV-7.1	353	87	115	5	0.00005	0.00075	0.3200 ± 0.0063	4.810 ± 0.101	0.10904 ± 0.00059	1789.5 ± 30.8	1783.4 ± 9.9	100.3
JHV-8.1	377	105	123	1	0.00001	0.00012	0.3193 ± 0.0079	4.819 ± 0.156	0.10949 ± 0.00196	1786.1 ± 38.8	1790.9 ± 33.0	99.7
JHV-9.1	178	273	78	2	0.00004	0.00058	0.3252 ± 0.0086	5.000 ± 0.188	0.11152 ± 0.00262	1814.8 ± 42.1	1824.4 ± 43.3	99.5
JHV-10.1	187	95	65	1	0.00001	0.00016	0.3198 ± 0.0078	4.887 ± 0.144	0.11082 ± 0.00152	1789.0 ± 38.3	1812.9 ± 25.1	98.7
JHV-11.1	123	83	44	0	0.00001	0.00016	0.3177 ± 0.0074	4.882 ± 0.123	0.11145 ± 0.00077	1778.3 ± 36.4	1823.2 ± 12.6	97.5
JHV-11.2R	293	88	98	0	0.00000	0.00004	0.3252 ± 0.0099	4.961 ± 0.154	0.11065 ± 0.00038	1815.1 ± 48.2	1810.1 ± 6.3	100.3
JHV-12.1	205	99	72	1	0.00002	0.00026	0.3279 ± 0.0109	4.896 ± 0.193	0.10832 ± 0.00187	1827.9 ± 53.3	1771.3 ± 31.9	103.2
JHV-13.1C[a]	475	50	188	32	0.00020	0.00321	0.3920 ± 0.0097	7.380 ± 0.209	0.13653 ± 0.00151	2132.3 ± 44.9	2183.7 ± 19.4	97.6
JHV-13.2R[a]	341	97	114	136	0.00144	0.02304	0.3150 ± 0.0072	5.144 ± 0.167	0.11843 ± 0.00242	1765.4 ± 35.3	1932.6 ± 37.0	91.3
JHV-14.1	340	111	114	1	0.00001	0.00016	0.3230 ± 0.0073	4.893 ± 0.117	0.10986 ± 0.00059	1804.6 ± 35.6	1797.0 ± 9.8	100.4
JHV-15.1[a]	692	531	235	139	0.00079	0.01270	0.2912 ± 0.0080	4.727 ± 0.173	0.11773 ± 0.00248	1647.4 ± 40.1	1922.1 ± 38.3	85.7
JHV-15.2	191	85	64	2	0.00003	0.00051	0.3150 ± 0.0072	4.747 ± 0.116	0.10930 ± 0.00070	1765.1 ± 35.4	1787.7 ± 11.8	98.7
W172-1.1	203	99	71	6	0.00010	0.00162	0.3258 ± 0.0066	4.879 ± 0.118	0.10862 ± 0.00116	1818.0 ± 32.3	1776.3 ± 19.6	102.3
W172-2.1[a]	449	123	130	74	0.00069	0.01097	0.2771 ± 0.0054	3.965 ± 0.100	0.10379 ± 0.00146	1576.5 ± 27.1	1693.1 ± 26.2	93.1
W172-3.1	248	121	84	4	0.00006	0.00088	0.3161 ± 0.0063	4.786 ± 0.109	0.10981 ± 0.00095	1770.6 ± 31.1	1796.3 ± 15.9	98.6
W172-4.1	199	88	67	8	0.00014	0.00224	0.3182 ± 0.0070	4.746 ± 0.126	0.10819 ± 0.00133	1780.7 ± 34.3	1769.2 ± 22.6	100.7
W172-5.1	260	84	87	5	0.00007	0.00105	0.3238 ± 0.0068	4.830 ± 0.121	0.10818 ± 0.00121	1808.3 ± 33.3	1769.0 ± 20.6	102.2
W172-6.1	196	81	66	6	0.00012	0.00191	0.3183 ± 0.0073	4.765 ± 0.123	0.10860 ± 0.00100	1781.2 ± 35.9	1776.1 ± 16.8	100.3
W172-7.1	167	69	57	9	0.00019	0.00307	0.3224 ± 0.0064	4.803 ± 0.116	0.10806 ± 0.00125	1801.3 ± 31.2	1767.0 ± 21.3	101.9
W172-8.1	141	85	51	1	0.00004	0.00058	0.3287 ± 0.0078	4.932 ± 0.138	0.10882 ± 0.00135	1832.2 ± 37.9	1779.8 ± 22.8	102.9
W172-10.1R	175	81	59	0	0.00001	0.00014	0.3146 ± 0.0074	4.764 ± 0.118	0.10983 ± 0.00064	1763.4 ± 36.3	1796.6 ± 10.6	98.1
W172-10.2C	271	107	94	11	0.00014	0.00229	0.3227 ± 0.0075	4.896 ± 0.121	0.11005 ± 0.00064	1802.8 ± 36.7	1800.3 ± 10.6	100.1
W172-11.1	166	49	54	0	0.00001	0.00016	0.3157 ± 0.0076	4.816 ± 0.123	0.11065 ± 0.00062	1768.5 ± 37.4	1810.1 ± 10.3	97.7
W172-12.1	206	79	69	0	0.00000	0.00004	0.3178 ± 0.0075	4.852 ± 0.119	0.11073 ± 0.00055	1778.8 ± 36.6	1811.4 ± 9.0	98.2
W172-13.1[a]	280	186	140	0	0.00000	0.00002	0.4289 ± 0.0181	9.180 ± 0.451	0.15524 ± 0.00319	2300.7 ± 82.1	2404.4 ± 35.3	95.7
W172-13.2R	196	83	69	1	0.00002	0.00027	0.3308 ± 0.0142	4.987 ± 0.221	0.10934 ± 0.00073	1842.2 ± 69.2	1788.4 ± 12.2	103.0
W172-14.1	154	86	54	0	0.00001	0.00016	0.3219 ± 0.0078	4.904 ± 0.125	0.11049 ± 0.00067	1799.0 ± 37.9	1807.5 ± 11.0	99.5
AMY-1.1	95	70	34	1	0.00003	0.00051	0.3134 ± 0.0076	4.748 ± 0.130	0.10988 ± 0.00109	1757.6 ± 37.5	1797.4 ± 18.1	97.8
AMY-2.1	90	84	34	0	0.00001	0.00016	0.3199 ± 0.0075	4.783 ± 0.118	0.10843 ± 0.00055	1789.4 ± 36.9	1773.2 ± 9.2	100.9
AMY-3.1	58	61	23	0	0.00001	0.00016	0.3187 ± 0.0083	4.834 ± 0.144	0.11001 ± 0.00126	1783.5 ± 40.6	1799.6 ± 21.0	99.1
AMY-3.2	137	201	58	0	0.00001	0.00018	0.3212 ± 0.0076	4.827 ± 0.129	0.10899 ± 0.00104	1795.7 ± 37.3	1782.7 ± 17.6	100.7
AMY-4.1	95	83	35	1	0.00004	0.00058	0.3117 ± 0.0076	4.738 ± 0.131	0.11024 ± 0.00111	1749.2 ± 37.6	1803.3 ± 18.5	97.0
AMY-5.1	102	96	39	0	0.00001	0.00016	0.3180 ± 0.0075	4.779 ± 0.119	0.10901 ± 0.00057	1779.9 ± 36.9	1782.9 ± 9.5	99.8
AMY-6.1C[a]	207	102	72	2	0.00003	0.00054	0.3203 ± 0.0224	4.830 ± 0.447	0.10938 ± 0.00573	1791.0 ± 110.4	1789.2 ± 98.6	100.1
AMY-6.2R	377	169	129	1	0.00001	0.00016	0.3206 ± 0.0076	4.844 ± 0.129	0.10957 ± 0.00106	1792.7 ± 37.0	1792.4 ± 17.8	100.0
AMY-7.1[a]	107	183	47	0	0.00002	0.00028	0.3113 ± 0.0074	4.805 ± 0.131	0.11194 ± 0.00117	1747.3 ± 36.6	1831.1 ± 19.1	95.4
AMY-8.1[a]	116	157	48	0	0.00002	0.00025	0.3177 ± 0.0076	4.900 ± 0.131	0.11186 ± 0.00104	1778.4 ± 37.5	1829.8 ± 16.9	97.2

Table 2 (Cont.)

Spot name	U (ppm)	Th (ppm)	Pb (ppm)	^{204}Pb (ppb)	^{204}Pb/^{206}Pb	f206	^{207}Pb/^{235}U	^{206}Pb/^{238}U	^{207}Pb/^{206}Pb	^{206}Pb/^{238}U Age (Ma)	^{207}Pb/^{206}Pb Age (Ma)	Conc. (%)
AMY-9.1	292	185	103	1	0.00001	0.00016	0.3166 ± 0.0081	4.730 ± 0.141	0.10834 ± 0.00134	1773.3 ± 39.8	1771.8 ± 22.8	100.1
AMY-10.1	122	155	48	1	0.00004	0.00058	0.3062 ± 0.0089	4.647 ± 0.149	0.11007 ± 0.00118	1722.1 ± 43.9	1800.6 ± 19.7	95.6
AMY-11.1	109	96	39	1	0.00004	0.00059	0.3046 ± 0.0073	4.627 ± 0.130	0.11018 ± 0.00130	1714.1 ± 36.4	1802.3 ± 21.6	95.1
AMY-12.1[a]	171	165	66	1	0.00002	0.00035	0.3220 ± 0.0085	4.745 ± 0.182	0.10688 ± 0.00266	1799.4 ± 41.4	1746.8 ± 46.2	103.0
W127-1.1	172	200	69	1	0.00003	0.00047	0.3206 ± 0.0058	4.809 ± 0.115	0.10877 ± 0.00147	1792.8 ± 28.4	1779.0 ± 24.9	100.8
W127-2.1	123	90	44	2	0.00006	0.00093	0.3118 ± 0.0042	4.683 ± 0.082	0.10892 ± 0.00106	1749.7 ± 20.6	1781.4 ± 17.8	98.2
W127-3.1	123	221	55	2	0.00005	0.00077	0.3166 ± 0.0082	4.718 ± 0.131	0.10808 ± 0.00074	1773.1 ± 40.5	1767.3 ± 12.6	100.3
W127-5.1	81	64	30	0	0.00001	0.00016	0.3220 ± 0.0047	4.855 ± 0.088	0.10936 ± 0.00102	1799.3 ± 22.8	1788.8 ± 17.1	100.6
W127-7.1	86	107	35	0	0.00001	0.00016	0.3188 ± 0.0049	4.775 ± 0.086	0.10863 ± 0.00086	1784.0 ± 23.8	1776.5 ± 14.5	100.4
W127-8.1	108	147	44	0	0.00001	0.00016	0.3145 ± 0.0046	4.761 ± 0.091	0.10981 ± 0.00115	1762.8 ± 22.6	1796.2 ± 19.2	98.1
W127-9.1	98	80	36	0	0.00001	0.00016	0.3163 ± 0.0065	4.758 ± 0.162	0.10910 ± 0.00268	1771.6 ± 32.1	1784.5 ± 45.5	99.3
W127-10.1	192	178	74	2	0.00004	0.00058	0.3226 ± 0.0100	4.839 ± 0.160	0.10879 ± 0.00088	1802.4 ± 48.9	1779.3 ± 14.9	101.3
W127-11.1	36	37	14	0	0.00001	0.00016	0.3187 ± 0.0056	4.865 ± 0.104	0.11069 ± 0.00114	1783.5 ± 27.2	1810.8 ± 18.9	98.5
W127-13.1	85	103	33	1	0.00004	0.00067	0.3070 ± 0.0044	4.702 ± 0.092	0.11107 ± 0.00131	1726.0 ± 21.7	1817.0 ± 21.6	95.0
W127-14.1	191	159	72	1	0.00003	0.00044	0.3220 ± 0.0034	4.865 ± 0.062	0.10958 ± 0.00064	1799.6 ± 16.5	1792.4 ± 10.7	100.4
W127-15.1	131	130	52	0	0.00001	0.00008	0.3258 ± 0.0040	4.971 ± 0.077	0.11068 ± 0.00091	1817.8 ± 19.4	1810.7 ± 15.0	100.4
W127-16.1[a]	144	150	55	1	0.00003	0.00041	0.3177 ± 0.0040	4.909 ± 0.110	0.11208 ± 0.00192	1778.4 ± 19.6	1833.4 ± 31.3	97.0
W127-17.1	101	93	38	0	0.00002	0.00025	0.3187 ± 0.0075	4.874 ± 0.133	0.11092 ± 0.00127	1783.3 ± 36.5	1814.5 ± 21.0	98.3
W127-18.1	119	135	47	0	0.00000	0.00004	0.3163 ± 0.0044	4.789 ± 0.089	0.10980 ± 0.00121	1771.8 ± 21.4	1796.0 ± 20.2	98.7
MCG-1.1	226	222	89	1	0.00001	0.00013	0.3209 ± 0.0047	4.846 ± 0.077	0.10953 ± 0.00070	1793.9 ± 23.0	1791.7 ± 11.6	100.1
MCG-2.1	298	220	112	7	0.00006	0.00086	0.3137 ± 0.0096	4.757 ± 0.148	0.10997 ± 0.00064	1782.0 ± 20.3	1798.9 ± 10.5	99.1
MCG-3.1	559	528	209	2	0.00001	0.00012	0.3184 ± 0.0041	4.830 ± 0.069	0.11003 ± 0.00068	1723.6 ± 12.7	1799.8 ± 11.2	95.8
MCG-4.1	114	82	42	3	0.00009	0.00133	0.3065 ± 0.0026	4.636 ± 0.060	0.10969 ± 0.00106	1768.4 ± 22.3	1794.2 ± 17.5	98.6
MCG-5.1	218	111	77	2	0.00003	0.00044	0.3157 ± 0.0046	4.760 ± 0.074	0.10936 ± 0.00061	1800.1 ± 13.0	1788.8 ± 10.2	100.6
MCG-6.1	341	159	115	2	0.00002	0.00031	0.3221 ± 0.0027	4.875 ± 0.057	0.10977 ± 0.00088	1709.4 ± 17.6	1795.5 ± 14.4	95.2
MCG-7.1	458	234	156	0	0.00000	0.00015	0.3037 ± 0.0036	4.607 ± 0.057	0.11001 ± 0.00041	1739.9 ± 9.5	1799.6 ± 6.7	96.7
MCG-8.1	245	155	86	0	0.00000	0.00015	0.3098 ± 0.0019	4.658 ± 0.041	0.10905 ± 0.00069	1701.9 ± 20.0	1783.6 ± 11.5	95.4
MCG-9.1	748	486	260	4	0.00002	0.00028	0.3021 ± 0.0040	4.574 ± 0.070	0.10980 ± 0.00083	1726.6 ± 13.8	1796.1 ± 13.6	96.2
MCG-10.1	269	236	99	0	0.00000	0.00015	0.3071 ± 0.0028	4.642 ± 0.093	0.10962 ± 0.00195	1759.0 ± 47.3	1793.2 ± 32.1	98.1

Uncertainties for zircon ^{206}Pb/^{238}U ratios do not include a component arising from calibration against the CZ3 zircon standard. Within a single analytical session, relative ^{206}Pb*/^{238}U ages of individual analyses are assessed correctly using their observed uncertainties, without calibration error included. When the uncertainty of an 'absolute' ^{206}Pb*/^{238}U age is reported for the mean of a group, it is necessary to add, in quadrature, the uncertainty (coefficient of variation) in the mean ^{206}Pb*/^{238}U determined for the CZ3 reference standard.

[a]Analysis omitted from calculation of mean age (see text).

geologically recent. The $^{207}Pb/^{206}Pb$ ratios for all analyses agree to within analytical precision, and yield a weighted mean of 0.10974 ± 0.00022, equivalent to 1795.1 ± 3.6 Ma (1σ). The best estimate of the crystallisation age of this sample is 1795 ± 8 Ma (95%, MSWD: 0.3).

Evaluation of results

A t-test statistical comparison of the results presented above shows that the only significant difference in means is between JHV and AMY (Table 3). As expected, means from the two samples of *in situ* upper June Hill Volcanics (JHV and W172) are indistinguishable, as are those from the dacitic porphyry east of Mt Amy (AMY and W127). Table 3 also shows t-test comparisons between each of our new ages and the recent SHRIMP age from the Capricorn Formation (Hall *et al*. 2001). In making these comparisons, we have used a weighted mean $^{207}Pb/^{206}Pb$ age for the Capricorn Formation of 1805.7 ± 6.6 Ma (95% conf.) as determined from the data presented in Hall *et al*. (2001). This Capricorn age is significantly different from both the unnamed dacitic porphyry and the Minnie Creek granite (AMY, W127, and MCG), but indistinguishable from the *in situ* upper June Hill Volcanics (JHV and W172).

The previous age of the June Hill Volcanics was reported as 1843 ± 2 Ma (Pidgeon & Horwitz 1991). The inheritance detected in this study—both in the new sample and re-examination of the Pidgeon and Horwitz concentrate—allows a reinterpretation of this age as one including an inherited component despite the best efforts of the previous analysts to avoid such natural contamination. With only a few analyses there is no discernible pattern to the inherited ages, although *ca* 1830 Ma ages are seen in both the AMY and W127 samples.

STRATIGRAPHIC IMPLICATIONS

The ages of the JHV and AMY samples are similar enough so that, if one proposed a protracted interval of June Hill-related volcanism, the porphyry could be considered as autochthonous June Hill Volcanics (Krapez 1997b, 1999) or as an olistolith reworked from the June Hill Volcanics (Pidgeon & Horwitz 1991 and references therein). The fact that our new age for the porphyry is precisely identical to that determined for the neighbouring Boolaloo Granodiorite (Krapez & McNaughton 1999) allows a third interpretation, that the porphyry is a shallow-level intrusion consanguineous with the underlying granodiorite (considered by Thorne & Seymour 1991: p. 88). If so, then lack of a contact aureole around the porphyry body implies intrusion at relatively shallow levels.

The June Hill Volcanics are similar in age to, if not slightly younger than, the lower, tuff-bearing part of the Capricorn Formation (1806 ± 7 Ma: recalculated from Hall *et al*. 2001). This presents a stratigraphic conundrum: south of the Paraburdoo Hinge Zone (Horwitz 1982) (Figure 1), the Capricorn Formation rests with angular unconformity above the Ashburton Formation, whereas in the Duck Creek synclinorium, the June Hill Volcanics lie unquestionably beneath what has been mapped as Ashburton Formation (Seymour *et al*. 1988). Accepting the SHRIMP zircon U–Pb ages from both the June Hill Volcanics (this study) and Capricorn Formation (Hall *et al*. 2001), the most reasonable solution is that what has been mapped as a single Ashburton Formation actually comprises two entirely distinct siliciclastic successions (Krapez & McNaughton 1999; Krapez 1999). The older Ashburton Formation lies in its type area along the Ashburton River drainage south of the Paraburdoo Hinge Zone: the younger 'Ashburton' succession is found north of Wyloo Dome, in the Duck Creek Synclinorium (Figures 1, 4). The discussion on turbidite sedimentation rates in the concluding statement by Hall *et al*. (2001) can now be amended as follows: the duration of type Ashburton sedimentation south of the Paraburdoo Hinge Zone is not tightly constrained, but the younger 'Ashburton' succession in the Duck Creek region was deposited entirely within an interval of about 10 million years.

These stratigraphic modifications are broadly similar to the model presented by Krapez (1999) and Krapez and McNaughton (1999) in that the Mininer and Wandarry Supersequences south of the Paraburdoo Hinge Zone were proposed to be older than the Cane River Supersequence most voluminously exposed north of Wyloo Dome, despite both successions being mapped as Ashburton Formation. Based on our new ages and comparisons with the age presented in Hall *et al*. (2001), we propose that the diachroneity in lithostratigraphy across the Wyloo Dome is even more pronounced: not just some, but all of the Ashburton Formation in the vicinity of the Capricorn Range is older than the so-called 'Ashburton' siliciclastic succession overlying the June Hill Volcanics in the Duck Creek Synclinorium (Figure 4). In the sequence-

Table 3 t-test comparisons between pairs of samples discussed in the text.

	JHV 1799 ± 8	W172 1797 ± 8	AMY 1786 ± 11	W127 1790 ± 10	MCG 1795 ± 8
JHV	–	–	–	–	–
W172	0.633	–	–	–	–
AMY	**0.030**	0.074	–	–	–
W127	0.123	0.258	0.518	–	–
MCG	0.427	0.750	0.131	0.416	–
Capricorn	0.200	0.081	**0.001**	**0.006**	**0.049**

Values are the t-distribution results calculated for unpaired two-tailed parametric tests assuming equal variance. **Bold** numbers indicate those comparisons where the null hypothesis, of both samples being drawn from the same population, can be rejected with >95% confidence. 'Capricorn' is our recalculated 1805.7 ± 6.6 Ma (95% conf.) age computed from the data tabulated by Hall *et al*. (2001)

stratigraphic terminology of Krapez (1999), we are therefore proposing that his Cane River Supersequence is not coeval with, but rather younger than, his Pingandy Supersequence.

An isochronous surface separating these two 'Ashburton' successions (*ca* 1807 Ma) would trace along the sub-Capricorn Formation unconformity in the Capricorn Range and reappear somewhere to the west of Wyloo Dome, then appear to cut downsection (in a lithostratigraphic sense) abruptly northward around the western nose of Wyloo Dome (Figure 1; see also Krapez 1999 figure 4). It is possible that the intraformational unconformity (McCarthy 2001) in the June Hill Volcanics, as presently defined, corresponds to this isochronous surface. In the vicinity of the Boolaloo Granodiorite, where the proposed unconformity intervenes between two deformed and contact-metamorphosed turbidite successions, its identification in the field may prove extremely challenging.

TECTONIC IMPLICATIONS AND MODEL

Can any of the three previously proposed tectonic models (Figure 2) be ruled out by our new SHRIMP ages? The Powell and Horwitz (1994) model of complete Wilson-cycle evolution between eruption of the June Hill Volcanics and deformation during the Capricorn Orogeny, was proposed at a time when the former were thought to be 1843 Ma (Pidgeon & Horwitz 1991) and the latter was thought to be dated by the syntectonic Boolaloo Granodiorite with Rb–Sr age of *ca* 1680 Ma (Leggo *et al.* 1965). Subsequent SHRIMP dating (Krapez & McNaughton 1999; this study) has now shown both units to be nearly synchronous, with mean ages separated by a mere 13 million years, and thus highly unlikely to bracket a complete Wilson cycle of continental-margin evolution. Numerical ages alone cannot distinguish between the other two models shown in Figure 2, as they both postulate convergent settings for the June Hill Volcanics and overlying Ashburton Formation.

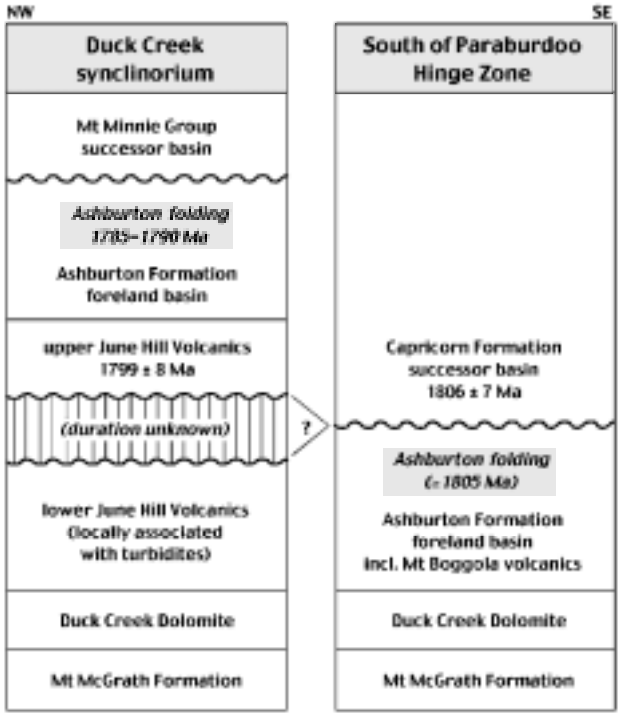

Figure 4 Chronostratigraphic implications of the new SHRIMP ages. See text for discussion and references.

Figure 5 depicts our vision of tectonic events in the Capricorn Orogen. Although arc–continental interactions at the northern margin of the Yilgarn Craton probably occupied an earlier interval of time (Figure 5a), we propose that this episode of tectonism bears its first manifestation in the Ashburton Fold Belt during deposition of the Duck Creek Dolomite. In that succession, a three-part stacking of basinal–platformal–basinal facies (Thorne & Seymour 1991) is interpreted here to indicate passing of a flexural forebulge through the southern Pilbara lithosphere. Depending on the orientation of loading and rate of hinterland convergence, these facies may be somewhat diachronous across the Ashburton Fold Belt. At the crest of the forebulge, platformal facies of the middle Duck Creek Dolomite are dominated by cyclic, metre-scale shallowing-upward sequences, each prograding/aggrading from subtidal to supratidal depositional environments (Thorne 1985). We hypothesise that these repetitive base-level changes may result primarily from the elastic response of the underthrusting Pilbara lithosphere to large-magnitude, characteristic thrust events in the northward-advancing Ashburton Fold Belt (Cisne 1986; Pratt *et al.* 1992). The broad deepening trend toward the upper Duck Creek Dolomite would then indicate the onset of direct flexural loading prior to basin infilling with Ashburton clastic sediments (Thorne & Seymour 1991). As discussed above, present numerical age constraints across the strike length of the Duck Creek Dolomite are inadequate to test the diachroneity of its drowning proposed here.

Thorne and Seymour (1991) postulated that the June Hill Volcanics erupted as a result of lithospheric flexure of the subducting Pilbara leading margin. Such a model is not without precedence: Hoffman (1987) identified five examples of foreland-basin mafic volcanism in Palaeoproterozoic orogens of the Canadian Shield. The lower part of the June Hill Volcanics is dominantly mafic (McCarthy 2001), most likely deposited on the outer ramp of the foredeep as indicated by conformity atop the drowned Duck Creek Dolomite platform. Above the intraformational unconformity, the upper part of the June Hill Volcanics (dated in this study) shows a different character: it is dominantly felsic and associated with 'Ashburton' (Cane River) turbidites bearing a magmatic-arc provenance (Thorne & Seymour 1991: pp. 73–81). Xenocrystic inheritance within the felsic June Hill zircon population indicates at least a minor cratonic contribution to this signature (Thorne & Seymour 1991: p. 81), but our new demonstration of coeval June Hill volcanism and Gascoyne plutonism (e.g. Minnie Creek granite) suggests that such a cratonic component may be overwhelmed by sources from the adjacent Gascoyne Province.

South of the Paraburdoo Hinge Zone, a 5–12 km-thick foreland wedge of Ashburton Formation clastic sediments was deposited (Thorne & Seymour 1991: p. 59), then

deformed into tight or isoclinal structures (Tyler & Thorne 1990), erosionally peneplained, and buried beneath successor sediments of the Capricorn Formation by 1806 ± 7 Ma (Hall *et al.* 2001). Typical foreland-basin infilling rates of 1–2 km/10^6 y (Chen *et al.* 2001) would suggest Ashburton sedimentation to occupy ~3–12 million years. Depending on the magnitude of depositional hiatus associated with folding and peneplanation beneath the sub-Capricorn unconformity, this would imply an age greater than *ca* 1820–1810 Ma for the base of the Ashburton Formation and hence the onset of flexural subsidence south of the Paraburdoo Hinge Zone. That estimated range is significantly older than our new age of 1799 ± 8 Ma from the upper June Hill Volcanics, which were deposited during the onset of foreland-basin sedimentation in the Duck Creek region. Such a northwest-younging diachroneity of similar tectonic processes occurred in conjunction with orogen-subparallel dextral shearing (Tyler & Thorne 1990), recently calibrated in the southern part of the Capricorn Orogen to 1810–1800 Ma (Occhipinti *et al.* 1998) (Figure 5b, c).

Based on the limited data available, late-stage granitoids in the Gascoyne Complex (Williams 1986) appear to young northward, from the 1800–1796 Ma neosomes in the southern part of the complex (Nelson 1995, 2000, 2001; Occhipinti *et al.* 1998) to the 1795 ± 8 Ma Minnie Creek Batholith (this study), to 1791 ± 10 Ma later phases of the Edmund Batholith (Pearson 1996), to the 1786 ± 5 Ma Boolaloo Granodiorite (Krapez & McNaughton 1999). Some of these igneous rocks are peraluminous, possibly of anatectic origin (Williams 1986), and it is tempting to speculate that the trend in ages represents advancement of a north-verging thrust stack.

Diachroneity in the Ashburton Fold Belt can be considered in the context of continued convergence and rotation generated by Pilbara indentation into the active Yilgarn margin. We suggest that by 1790 Ma, as Pilbara collision continued to indent the Yilgarn hinterland, the Ashburton Fold Belt and Gascoyne block accommodated strain via dextral shear (Tyler & Thorne 1990; Occhipinti *et al.* 1998) and rotation around the Wyloo Dome (Figure 5d), possibly incorporating some lateral extrusion of the Gascoyne Province (Tyler & Thorne 1990). Foreland-basin infilling of the Cane River succession northwest of Wyloo Dome was a response to lithospheric loading associated with dextral transpression in that region. A modern

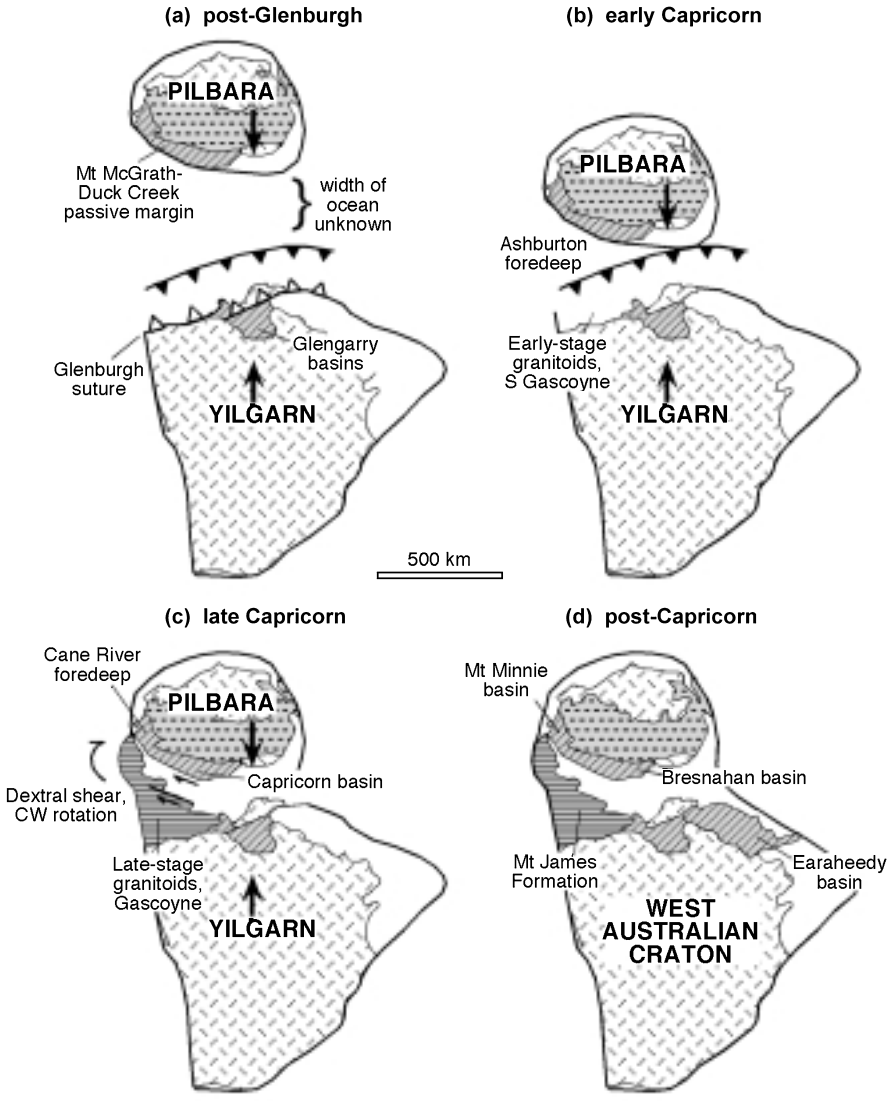

Figure 5 Plate-tectonic model of late orogenic events in the Capricorn Orogen. Patterns represent present exposure of Archaean cratons (cross-hatched), Neoarchaean to earliest Palaeoproterozoic cover (dashed), Late Palaeoproterozoic cover (diagonally ruled), Late Palaeoproterozoic igneous–metamorphic complex (horizontally ruled), and cover not yet deposited at time shown (white). (a) 1950–1850 Ma, following cessation of the Glenburgh Orogeny (Occhipinti *et al.* 1999). (b) 1830–1810 Ma, first contact between Pilbara and Yilgarn Cratons. The older age limit of *ca* 1830 Ma is estimated based on typical rates of foreland-basin evolution. (c) 1805–1785 Ma, continued indentation of Pilbara, dextral shear and late-stage granitisation within Gascoyne internal zone. (d) 1785– 1700 Ma, successor basin development with final stages of orogenesis.

analogy, with similar kinematics (geographically inverted to the Capricorn example) but at a larger scale, may be found at the Burma–Yunnan syntaxis of the India–Asia collision, where clockwise rotation of the upper plate about the syntaxis (England & Molnar 1990) is linked with dextral transpression following east–west shortening in the northern Indo-Burman Ranges (Ni *et al.* 1989). If these (inverted) analogous kinematics may be extrapolated northward along the western Pilbara margin, then the recently documented east–west convergence in the Cape Preston area (directly north of the northernmost Wyloo Group exposures in Figure 1) may be related to the Capricorn Orogeny rather than a separate collision with another plate (Hickman & Strong 1998).

ACKNOWLEDGEMENTS

Thanks to Matt Baggott and Marion Marshall for careful and efficient zircon separation. Ian Tyler, Allan Thorne, and David Martin are thanked for discussions, as are Alec Trendall and an anonymous referee for their thoughtful reviews of the manuscript. The late Chris Powell gave logistical support, engaging discussions, and many fond Pilbara memories. This research is supported by ARC Postdoctoral Fellowships to DADE, MTDW and KNS and a Small Grant to DADE. Zircon analyses were performed at the Western Australian SHRIMP facilities operated by a Western Australian university–government consortium with ARC support. Tectonics Special Research Centre contribution 231.

REFERENCES

CHEN W-S., RIDGWAY K. D., HORNG C-S., CHEN Y-G., SHEA K-S. & YEH M-G. 2001. Stratigraphic architecture, magnetostratigraphy, and incised-valley systems of the Pliocene–Pleistocene collisional marine foreland basin of Taiwan. *Geological Society of America Bulletin* **113**, 1249–1271.

CISNE J. L. 1986. Earthquakes recorded stratigraphically on carbonate platforms. *Nature* **323**, 320–322.

CLAOUÉ-LONG J. C., COMPSTON W., ROBERTS J. & FANNING C. M. 1995. Two Carboniferous ages: a comparison of SHRIMP zircon ages with conventional zircon ages and $^{40}Ar/^{39}Ar$ analysis. *In:* Berggren, W. A., Kent, D. V., Aubrey, M.-P. & Hardenbol, J. eds. *Geochronology, Time Scales, and Global Stratigraphic Correlation*, pp. 3–21. Society of Economic Paleontologists and Mineralogists Special Publication **54**.

COMPSTON W., WILLIAMS I. S., KIRSCHVINK J. L., ZHANG Z. & MA G. 1992. Zircon U–Pb ages for the Early Cambrian time-scale. *Journal of the Geological Society of London* **149**, 171–184.

COMPSTON W., WILLIAMS I. S. & MEYER C. 1984. U–Pb geochronology of zircons from lunar breccia 73217 using a sensitive high mass-resolution ion microprobe. *Journal of Geophysical Research Supplement* **89**, B525–B534.

CUMMING G. L. & RICHARDS J. R. 1975. Ore lead isotope ratios in a continuously changing Earth. *Earth and Planetary Science Letters* **28**, 155–171.

ENGLAND P. & MOLNAR P. 1990. Right-lateral shear and rotation as the explanation for strike-slip faulting in eastern Tibet. *Nature* **344**, 140–142.

GEE R. D. 1979. Structure and tectonic style of the Western Australian Shield. *Tectonophysics* **58**, 327–369.

HALL C. E., POWELL C. MCA. & BRYANT J. 2001. Basin setting and age of the Late Proterozoic Capricorn formation, Western Australia. *Australian Journal of Earth Sciences* **48**, 731–744.

HICKMAN A. H. & STRONG C. A. 1998. Structures in the Cape Preston area, northwestern Pilbara Craton: new evidence for a convergent margin. *Geological Survey of Western Australia Annual Review 1997–98*, 77–84.

HOFFMAN P. F. 1987. Early Proterozoic foredeeps, foredeep magmatism, and superior-type iron-formations of the Canadian Shield. *In:* Kröner, A. ed. *Proterozoic Lithospheric Evolution*, pp. 85–98. American Geophysical Union Geodynamics Series **17**.

HORWITZ R. C. 1982. Geological history of the early Proterozoic Paraburdoo Hinge Zone, Western Australia. *Precambrian Research* **14**, 191–200.

KRAPEZ B. 1997a. Sequence-stratigraphic concepts applied to the identification of depositional basins and global tectonic cycles. *Australian Journal of Earth Sciences* **44**, 1–36.

KRAPEZ B. 1997b. Reply. Sequence-stratigraphic concepts applied to the identification of depositional basins and global tectonic cycles. *Australian Journal of Earth Sciences* **44**, 879–886.

KRAPEZ B. 1999. Stratigraphic record of an Atlantic-type global tectonic cycle in the Palaeoproterozoic Ashburton Province of Western Australia. *Australian Journal of Earth Sciences* **46**, 71–87.

KRAPEZ B. & MCNAUGHTON N. J. 1999. SHRIMP zircon U–Pb age and tectonic significance of the Palaeoproterozoic Boolaloo Granodiorite in the Ashburton Province, Western Australia. *Australian Journal of Earth Sciences* **46**, 283–287.

LEGGO P. J., COMPSTON W. & TRENDALL A. F. 1965. Radiometric ages of some Precambrian rocks from the Northwest Division of Western Australia. *Journal of the Geological Society of Australia* **12**, 53–65.

MARTIN D. MCB., LI Z. X., NEMCHIN A. A. & POWELL C. MCA. 1998. A pre-2.2 Ga age for giant hematite ores of the Hamersley Province, Australia? *Economic Geology* **93**, 1084–1090.

MARTIN D. MCB., POWELL C. MCA. & GEORGE A. D. 2000. Stratigraphic architecture and evolution of the early Paleoproterozoic McGrath Trough, Western Australia. *Precambrian Research* **99**, 33–64.

MCCARTHY M. 2001. Physical volcanology, tectonic framework and palaeomagnetism of the June Hill Volcanics, Ashburton Basin, Western Australia. BSc (Hons) thesis, University of Western Australia, Perth (unpubl.).

NELSON D. R. 1995. Compilation of SHRIMP U–Pb zircon geochronology data, 1994. *Geological Survey of Western Australia Record* **1995/3**.

NELSON D. R. 1997. Compilation of SHRIMP U–Pb zircon geochronology data, 1996. *Geological Survey of Western Australia Record* **1997/2**.

NELSON D. R. 1998. Compilation of SHRIMP U–Pb zircon geochronology data, 1997. *Geological Survey of Western Australia Record* **1998/2**.

NELSON D. R. 1999. Compilation of SHRIMP U–Pb zircon geochronology data, 1998. *Geological Survey of Western Australia Record* **1999/2**.

NELSON D. R. 2000. Compilation of SHRIMP U–Pb zircon geochronology data, 1999. *Geological Survey of Western Australia Record* **2000/2**.

NELSON D. R. 2001. Compilation of SHRIMP U–Pb zircon geochronology data, 2000. *Geological Survey of Western Australia Record* **2001/2**.

NI J. F., GUZMAN-SPEZIALE M., BEVIS M., HOLT W. E., WALLACE T. C. & SEAGER W. R. 1989. Accretionary tectonics of Burma and the three-dimensional geometry of the Burma subduction zone. *Geology* **17**, 68–71.

OCCHIPINTI S. A., SHEPPARD S., NELSON D. R., MYERS J. S. & TYLER I. M. 1998. Syntectonic granite in the southern margin of the Palaeoproterozoic Capricorn Orogen, Western Australia. *Australian Journal of Earth Sciences* **45**, 509–512.

OCCHIPINTI S. A., SHEPPARD S., TYLER I. M. & NELSON D. R. 1999. Deformation and metamorphism during the c.2000 Ma Glenburgh Orogeny and c.1800 Ma Capricorn Orogeny. *Geological Society of Australia Abstracts* **56**, 26–29.

PEARSON J. M. 1996. Alkaline rocks of the Gifford Creek Complex, Gascoyne Province, Western Australia: their petrographic and tectonic significance. PhD thesis, University of Western Australia, Perth (unpubl.).

PIDGEON R. T., FURFARO D., KENNEDY A. K., NEMCHIN A. A. & VAN BRONSWIJK W. 1994. Calibration of zircon standards for the Curtin SHRIMP II. *Abstracts of the 8th International Conference on*

Geochronology, Cosmochronology and Isotope Geology, Berkeley, USA, p. 251. US Geological Survey Circular 1107.

PIDGEON R. T. & HORWITZ R. C. 1991. The origin of olistoliths in Proterozoic rocks of the Ashburton Trough, Western Australia, using zircon U–Pb isotopic characteristics. *Australian Journal of Earth Sciences* **38**, 55–63.

POWELL C. MCA. & HORWITZ R. C. 1994. Late Archaean and Early Proterozoic tectonics and basin formation of the Hamersley Ranges. *12th Australian Geological Convention, Perth, Excursion Guidebook* **4**.

PRATT B. R., JAMES N. P. & COWAN C. A. 1992. Peritidal carbonates. *In:* Walker, R. G. & James, N. P. eds. *Facies Models: Response to Sea Level Change*, pp. 303–322. Geological Association of Canada GEOtext **1**.

SEYMOUR D. B., THORNE A. M. & BLIGHT D. F. 1988. Wyloo. WA (2nd edition). *Geological Survey of Western Australia 1:250 000 Geological Series Explanatory Notes.*

STEIGER R. H. & JÄGER E. 1977. Subcommission on geochronology: convention on the use of decay constants in geo- and cosmochronology. *Earth and Planetary Science Letters* **36**, 359–362.

THORNE A. M. 1985. Upward-shallowing sequences in the Precambrian Duck Creek Dolomite, Western Australia. *Geological Survey of Western Australia Report* **14**, 81–93.

THORNE A. M. & SEYMOUR D. B. 1991. Geology of the Ashburton Basin, Western Australia. *Geological Survey of Western Australia Bulletin* **139**.

TYLER I. M. & THORNE A. M. 1990. The northern margin of the Capricorn Orogen, Western Australia – an example of and Early Proterozoic collision zone. *Journal of Structural Geology* **12**, 685–701.

WILLIAMS S. J. 1986. Geology of the Gascoyne Province, Western Australia. *Geological Survey of Western Australia Report* **15**.

Received 20 January 2003; accepted 22 August 2003